

EoC: Improving Cellular Access Mapping through Evidence of Coverage

Anonymous Author(s)

ABSTRACT

Understanding and improving mobile broadband deployment is critical to bridging the digital divide and targeting investments. In 2019, the Federal Communications Commission (FCC) released a report on the progress of mobile broadband deployment in the United States [10]. This report received a significant amount of criticism with claims that LTE coverage was over-reported in certain areas [23]. We evaluate the validity of this criticism using a quantitative analysis of both the dataset from which the FCC based its report [9] and a crowdsourced LTE coverage dataset [53]. Our findings reveal that there is significant disagreement between the crowdsourced dataset and the FCC dataset regarding the presence of LTE coverage in rural and tribal census blocks, with disagreement in up to 15% of these census blocks. Based on these findings and the challenges of generating ground truth LTE coverage data at scale, we formalize the value of new measurements by introducing *evidence of coverage* (EoC), a geospatial metric that enables multiple coverage data sets to be integrated with additional data so that communities can leverage a *targeted active measurement framework* to craft resource-optimized measurement campaigns.

1 INTRODUCTION

Affordable, quality Internet access is critical for full participation in the 21st century economy, education system, and government access [49, 50]. Worldwide, Internet access has become increasingly available through mobile broadband LTE cellular networks [28–30]. In the United States, cellular operators have expanded and upgraded their networks to LTE [13–15, 17], and 5G is now on the horizon. However, this expansion is often guided by economic demand, concentrating deployment in urban areas and leaving economically marginalized and sparsely populated areas underserved [17].

To address these digital inequities, the U.S. government has introduced incentive programs to offset the costs for LTE operators to build infrastructure to serve rural areas [16, 47]. The Federal Communications Commission (FCC) collects network connectivity reports from commercial network operators across the United States and allocates funds to cover regions that are not served by any commercial LTE operators. To keep the process transparent, the FCC makes LTE coverage data public by releasing shapefiles for each operator indicating geographic areas of coverage [19]. However, following the release of successive broadband improvement

reports, various claims have been made challenging the veracity of the data presented [3, 33, 51]. For example, recently the Rural Wireless Association claimed that Verizon overestimates LTE coverage by a factor of two in the Oklahoma Panhandle [51]; other examples are considered in Section 5.

This over-reporting can be attributed to the proprietary and often generous propagation models used by network operators [23]. As dependence on mobile broadband connectivity increases, alternate methodologies are becoming acutely necessary to evaluate and direct resources in Internet access deployment efforts [46].¹ Thus, beyond the existence of over-reporting (which is relatively well-established), the need exists to identify specific locations where FCC coverage data is likely to be inaccurate and to provide evidence that states and communities can use to advocate for resources. While individual communities can conduct some of this work themselves, it is time-intensive, requires technical know-how, and may lack the objectivity that can be provided by third-party analysis.

The goal of this paper is to characterize LTE coverage in the United States by examining multiple coverage datasets that have been constructed independently and use these imperfect datasets to propose specific methods that improve coverage maps via targeted measurement campaigns.

Current LTE coverage measurement methodologies, apart from network operator reports, can be broadly classified into two categories: crowdsourced and ground truth². Crowdsourced measurements are contributed by users on the LTE network, so the geographical scope of the measurements is limited by user participation in an area. Ground truth measurement uses specialized equipment with dedicated users (e.g., wardriving [27]). This method allows greater control over the measurement metric and the geographic scope, but does not scale due to high economic and labor costs. Given

¹We note that *access* and *adoption* are different. Several studies demonstrate that even where mobile broadband is available, it is not necessarily adopted due to factors such as cost of devices, service fees, lack of perceived utility and relevance, and societal barriers (e.g. gendered restrictions) [30, 31, 45]. Understanding these factors, however, is outside the scope of this paper.

²We recognize that crowdsourced measurements could also be construed as ground truth. However, as we will show later in the paper, these measurements are used as input to propagation and coverage models for cell towers, which in some cases leads to coverage calculation errors. Hence they are not “ground truth” per se. On the other hand, when we say “ground truth” in this paper, we mean intentional measurements that record coverage and coverage quality in a given location.

the difference in characteristics of these methods, this paper considers a specific crowdsourced coverage dataset used by Skyhook, a commercial location service provider, as well as ground truth data collected via our own active measurement campaign with a smaller geographic scope.

Our initial analysis compares coverage maps and ground truth measurements in New Mexico, which we selected for its mix of demographics, diverse geographic landscape, and our partnership with community stakeholders within the state [41, 58]. Our analysis is guided by the following question: (i) *How consistent are existing LTE coverage datasets*, (ii) *Where and how do their coverage estimations differ?* We do a statewide coverage comparison between the FCC and the Skyhook LTE coverage datasets and find interesting differences in reported coverage, especially in rural and tribal areas. We then compare these coverage datasets against the ground truth dataset and find that both of them tend to overestimate coverage.

We find that the FCC LTE coverage dataset is more likely to be accurate in some areas than others. While crowdsourced coverage measurements can provide evidence that supports or discredits the accuracy of the FCC LTE coverage data, crowdsourced measurements are notorious for being sparse in the areas that are most likely to be inaccurately reported as covered (i.e., rural and tribal areas). Thus, in order to gather evidence that accurately reflects the state of LTE coverage, underserved communities need to be able to collect targeted coverage data through intentional measurement efforts. The collection of meaningful ground-truth coverage data is non-trivial due to resource limitations. In investigating a solution for determining *where to measure next*, we are guided by the following questions: (i) *Where are we most (and least) confident in the accuracy of LTE coverage data?*; and (ii) *Given a resource budget, how do we determine which locations are most valuable for a targeted ground-truth measurement campaign?*

To this end, we propose a solution that enables communities, or others with available resources, to identify the places where measuring LTE coverage yields the highest gain in terms of increasing evidence about the state of coverage. Policy input on the value of better understanding, such as the population of the region, can also be incorporated into the model. The key idea is to use existing datasets to assign “evidence of coverage” to locations in the geographic region of interest, reflecting whether the data indicates the region is covered or uncovered and with what measure of certainty. We then frame the problem of determining where to collect new LTE coverage data as a cost-constrained traveling salesman problem (TSP) with a utility assigned to visiting each node and an overall budget that limits the possible size of the tour [54]. In this framework, nodes are grid blocks that may produce a ground measurement with a utility; block utilities are determined by the amount of evidence as well as

Data Set	Points of Collection	Format	Methodology
FCC	Polygon overlay	Shapefile	Operator-reported with Form 477
Skyhook	Cell signal point	CSV	Incidental crowdsourcing
Author Ground Measurements	Cell signal point	CSV	Wardriving

Table 1: Summary of coverage data sets.

the value that ground measurement at that block would add to the overall coverage map; and the cost of visiting each block is determined by budgetary factors, such as travel time and distance, which limits the total number of blocks able to be visited in a TSP tour.

Our findings and contributions are summarized as follows:

- (1) FCC LTE coverage maps tend to disagree most with the crowdsourced coverage measurements in rural areas, reporting coverage in as many as 15% *more* rural New Mexico census blocks for some network operators.
- (2) Both FCC and crowdsourced datasets report higher coverage relative to our ground truth measurements. However, the FCC dataset shows a higher degree (by up to 26.7%) of over-reporting than the crowdsourced dataset.
- (3) By accumulating evidence of coverage from a variety of sources, we demonstrate how even imperfect data can be leveraged to determine where additional ground truth measurements are most needed.
- (4) We demonstrate how our novel approach to mapping evidence of coverage enables the development of targeted measurement campaigns that balance a variety of resource constraints.

The remainder of the paper is organized as follows: Section 2 explains the datasets. Analysis of LTE coverage data is presented in Section 3. The evidence of coverage metric and corresponding map, as well as the targeted active measurement framework, are described in Section 4. Section 5 gives an overview of the related work. Section 6 discusses recommendations, future work, and concludes the paper.

2 DATASETS

In this section we first describe the geographic scope of our study, followed by a description of each of the LTE coverage datasets we use. These datasets are summarized in Table 1. We also highlight the limitations associated with each data collection methodology.

2.1 FCC Dataset

The FCC LTE broadband dataset consists of coverage shapefiles that depict geospatial LTE network deployment for the cellular operators in the United States. The FCC compiles this dataset semi-annually from operators through Form 477 [20]. Every cellular operator that owns cellular network facilities

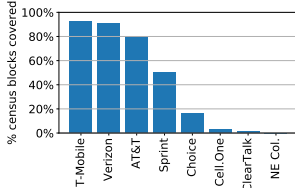


Figure 1: LTE operators by census block coverage.

must participate in this data collection. The operators submit detailed network information in the form of geo-polygons along with the frequency band used in the polygon and the minimum advertised upload and download speeds. The methodology used for obtaining these polygons is proprietary to each operator. In the end, the FCC makes publicly available only a coverage map that represents coverage as binary; there either is or is not cellular service. We use the latest binary coverage shapefiles, available on the FCC’s website, from December 31, 2018 [9]. Figure 1 shows the eight LTE network operators present in the state of New Mexico (NM) and the percentage of total census blocks in NM covered by each operator. Note that a census block is considered covered if the centroid of the census block is covered [18]. In this paper, we limit our analysis to data involving performance of the top four cellular operators due to their significantly greater prevalence in NM; these operators are also the top four cellular operators in the United States more broadly.

Limitations: These coverage maps are generated using models that are proprietary to the operator [23]. Furthermore, the publicly available dataset only consists of binary coverage and the FCC does not provide performance-related data.

2.2 Skyhook Dataset

Skyhook is a location service provider that uses a variety of positioning tools, including a database of cell locations to offer precise geolocation to subscribed applications [53]. Through apps that subscribe to Skyhook’s location services, user devices report back network information, which is gathered into anonymous logs and used to further improve the localization service. Through a data access agreement we are able to view two types of datasets from Skyhook: *scan logs* from user equipment (UE) and a *cell location database*.

The scan logs are measurements gathered by UEs using the Skyhook API for localization. These consist of the unique ID of the cell to which the UE is connected, the geolocation of the UE, and the associated signal strength, i.e., Reference Signal Received Power (RSRP). Other metadata, such as the timestamp of measurement, device type, and cell technology (i.e., LTE or UMTS(3G)) are also present.

The cell location database is a list of unique LTE cell base station IDs along with the cell technology, estimated location, and the estimated coverage. The database was originally constructed through extensive wardriving but is now managed

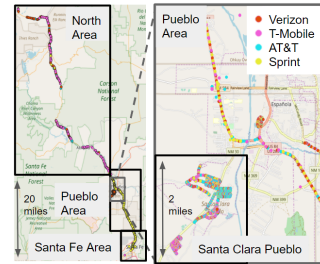


Figure 2: Map of author wardriving areas in New Mexico.

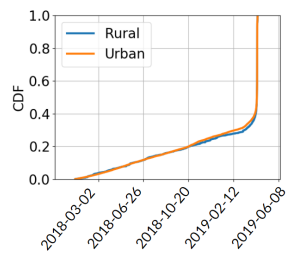


Figure 3: CDF of cell updates in Skyhook rural and urban measurements.

and updated using the scan logs dataset. Scan logs with the same cell ID are combined to estimate the cell location and coverage in the following manner:

Cell location estimation: A grid-based methodology similar to that proposed by Nurmi et al. [42] is used to estimate the cell tower location. Specifically, Skyhook divides the geographic area into 7 m squares and groups measurements in the same square to obtain a central measure of the square’s signal strength. This is done to reduce the bias due to large numbers of measurements coming from the same area (e.g. a popular gathering place). A weighted average of the signal strength is then used to estimate the cell location.

Estimation of cell coverage radius: Skyhook also provides an estimate of the cell’s coverage radius using a proprietary method based on the path-loss gradient [55]. The value of the path-loss gradient depends on several factors such as environment (urban vs rural), geographic topography, and cell signal frequency. Skyhook estimates the path-loss gradient using field observations of cell signal strength readings along with their distributed geographic locations. Ideally, the path loss varies based on the direction and the distance from the cell. However, to reduce the complexity of coverage estimation, Skyhook’s cell coverage estimation heuristic calculates only one path-loss gradient for a single cell. The path-loss gradient is then used in a set of parameterized equations to estimate the cell coverage radius. The parameters in these equations have been determined with careful research and testing over more than 10 years.

The cell location database is updated regularly with recalculation of cell location and cell coverage radius using the new scan logs that have been collected since the last update. For our analysis, we use the cell location database last updated on April 30, 2019.

Limitations: Since database entries are crowdsourced from UEs when the device passes within range of a cell, this dataset is more comprehensive in population centers and highways where people more often frequent. If there are too few measurements overall, or if measurements are primarily sourced from the same grid section, then the cell location estimate can be inaccurate.

2.3 Ground Measurement Campaign

To complement these datasets, we performed a targeted measurement campaign to collect driving ground truth measurements through 120 miles of Rio Arriba county in New Mexico over a period of five days beginning May 28, 2019. Figure 2 shows the locations of ground measurements and the four descriptive area labels we use for this analysis. The North area measurements were taken on highways passing primarily through national forest. The Pueblo area measurements were taken from highways within tribal jurisdiction boundaries. In Santa Clara Pueblo, tribal leadership permitted us to collect additional measurements in residential zones. Finally, the Santa Fe area consists of highway measurements between the pueblos and downtown Santa Fe. While limited in scale, these ground measurements provide an important comparison point for actual coverage and user experience, particularly because prior studies show that FCC coverage data tends to be overstated [23, 33, 51]. As described in Section 1, we selected these areas of New Mexico for their mix of tribal and non-tribal demographics; tribal lands tend to have the highest coverage over-statements and the most limited cellular availability within the United States [14, 15, 17].

Our ground measurements consist of *service state* and signal strength readings recorded on four Motorola G7 Power (XT1955-5) phones running Android Pie (9.0.0). *Service State* is a discrete variable indicating whether the phone is connected to a cell. Measurements were collected using the *Network Monitor* application [37]. An external GlobalSat BU-353-S4 GPS connected to an Ubuntu Lenovo ThinkPad laptop gathered geolocation tags that were matched to network measurements by timestamp. Each phone was outfitted with a SIM card from one of the four top cellular operators in the area: Verizon, T-Mobile, AT&T, and Sprint. The phones recorded service state and signal strength every 10 seconds while we drove at highway speeds (between 40 and 65 miles per hour) in most places and less than 10 miles per hour in residential areas (Santa Clara Pueblo).

Limitations: Our wardriving campaign was intensive in terms of human effort, economic cost, and time, making it difficult to scale. The dataset does not capture any temporal variations in coverage as the measurements were collected over a short span of time.

2.4 Statement of Ethics

The Skyhook data we use in this paper has been collected by Skyhook with user consent. Given the low population density associated with locations where we focus our analysis, privacy of network users is a concern. While scan logs are anonymized, we note that we also make no effort to link separate measurements to the same user, as this could potentially reveal unique identities of users who have unusual

access patterns. Taking a broader view of ethics, our work has the potential for positive impact on society because it focuses on universal access and disparities that may correlate with rural and/or tribal geographies.

3 ANALYSIS

In this section we examine the extent to which the LTE datasets present a similar picture of coverage.

3.1 Comparison of Coverage

We compare LTE coverage across three datasets: FCC, Skyhook, and ground truth measurements. We focus on the state of New Mexico as our ground measurement area for its diverse geographic landscapes and political jurisdictions [41, 58]. In all cases, however, our methodology is generalizable.

3.1.1 Coverage comparison between the FCC and Skyhook. We first compare a coverage shapefile generated from Skyhook cell locations and estimated coverage ranges with the FCC map for each operator.

Methodology: We consider coverage at the census block level for this comparison. In addition to reporting coverage shapefiles, the FCC reports coverage at a census block level and considers a census block as covered if the centroid of the census block falls within a covered region [18]. We generate a similar census block level coverage map per-operator using Skyhook’s estimated coverage. To do so, we first obtain the coverage shapefile for each operator using a cell’s estimated location and coverage radius. Then we use the FCC centroid methodology to generate the Skyhook LTE coverage map at the census block level. We use the Python geopandas library for the associated spatial operations [21]. We group census blocks into four categories: non-tribal urban (NT_U), non-tribal rural (NT_R), tribal urban (T_U), and tribal rural (T_R). This is done to explore whether the degree of agreement of the two datasets varies across these dimensions. We use the U.S. Census Bureau’s classification of urban and rural blocks and its boundary definitions of tribal jurisdiction for this categorization [7]. In this analysis we consider census blocks as tribal if they overlap with any tribal boundaries.

Results: Table 2 shows the percentage of total census blocks covered by each cellular operator, according to the FCC and Skyhook data, broken down by census block type. Among the four operators, T-Mobile covers the greatest number of census blocks based on both FCC and Skyhook data, while Sprint covers the fewest. All four cellular operators have relatively higher coverage for both tribal and non-tribal urban census blocks. However, all operators except Verizon offer their lowest coverage in tribal rural areas. In some cases, the differences between non-tribal rural (NT_R) and tribal rural (T_R) are as great as 23%.

Census block type	Total census blocks	Verizon		T-Mobile		AT&T		Sprint	
		FCC	Skyhook	FCC	Skyhook	FCC	Skyhook	FCC	Skyhook
NT_R	93680	89%	77%	94%	86%	84%	79%	38%	49%
NT_U	41872	100%	100%	100%	100%	100%	99%	96%	99%
T_R	30588	91%	83%	90%	63%	81%	74%	26%	41%
T_U	2469	100%	100%	94%	94%	94%	74%	74%	88%
All	168609	92%	84%	95%	86%	88%	83%	51%	61%

Table 2: Percentage of total census blocks covered according to FCC and Skyhook.

Block type	Total blocks	Verizon	T-Mobile	AT&T	Sprint
NT_R	93680	13974	8909	8276	1162
NT_U	41872	0	0	217	25
T_R	30588	4020	8480	3448	220
T_U	2469	0	0	2	0

Table 3: Number of census blocks where there is coverage according to FCC but no coverage according to Skyhook.

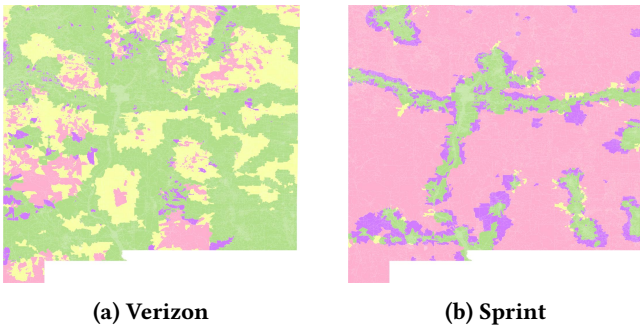


Figure 4: Comparison of LTE coverage maps of New Mexico. Yellow blocks are covered in the FCC map but not in Skyhook; purple blocks are covered in the Skyhook map but not the FCC. Green blocks are covered in both, and pink blocks are covered in neither.

The extent of LTE coverage differs between the two datasets. For three out of four providers, Skyhook shows lower coverage than the FCC, particularly in the rural census blocks. For instance, the FCC T-Mobile data shows coverage in 90% of tribal rural blocks, whereas Skyhook shows coverage in only 63% of such blocks. On the other hand, Skyhook shows a higher number of census blocks covered than the FCC for Sprint. We believe this could be because the Skyhook coverage map data was updated in June 2019, whereas the FCC coverage maps correspond to December 2018. Network operators could have expanded service in that time period. Figure 4 visually compares the LTE coverage maps from the FCC and the Skyhook datasets for Verizon and Sprint.

We more deeply examine the discrepancy mapped in yellow in Figure 4a. Table 3 shows the number of census blocks where there is coverage according to the FCC but none according to Skyhook for each operator. Coverage claims in both tribal and non-tribal rural census blocks disagree the most. The number of such blocks are particularly high for

Block type	Verizon	T-Mobile	AT&T	Sprint
NT_R	528 (1%)	2,635 (3%)	5,329 (6%)	20 (<1%)
NT_U	0 (0%)	0 (0%)	217 (1%)	0 (0%)
T_R	2,655 (9%)	2,486 (8%)	2,548 (8%)	0 (0%)
T_U	0 (0%)	0 (0%)	2 (<1%)	0 (0%)

Table 4: Number of census blocks with LTE coverage according to the FCC, but only 3G coverage according to Skyhook. The numbers in parenthesis report the same data as a percentage of total census blocks of the corresponding type.

Verizon (17,994 in total) and T-Mobile (17,389). There are two possible reasons for this disagreement: i) network operators lack infrastructure in rural areas, but tend to overestimate coverage while reporting it to FCC, or ii) Skyhook is missing data points from rural census blocks where fewer people carry UEs that detect the presence of LTE cells.

To understand which of these potential reasons for disagreement is more likely true, we check whether Skyhook shows 3G coverage for these census blocks (where the FCC reports LTE coverage but Skyhook does not). If Skyhook reports 3G coverage in these blocks, this confirms that users have contributed to the Skyhook dataset in these census blocks, therefore LTE coverage would have been detected if it existed. We generate a 3G coverage map at the census block level for these areas in the same manner as described previously. The number of census blocks that show only 3G coverage according to Skyhook is presented in Table 4. We observe a significant number of census blocks where Skyhook detects 3G coverage, indicating that in these areas it is likely the FCC LTE coverage claims are overstated. The number of such blocks is greater for tribal rural areas (up to 9%), thus indicating a higher mismatch of the two datasets in tribal rural areas.

3.1.2 Ground truth data compared to FCC and Skyhook coverage. In this section, we compare our own ground truth measurements with the coverage maps from the FCC and Skyhook described in Section 3.1.1. We focus now on the geographic region around Santa Clara Pueblo, which lies north of Santa Fe (see Figure 2), a region with a mix of urban, rural, and tribal population blocks.

Methodology: We use the *Service State* readings collected in our ground measurements for this analysis (see Section 2.3). We also collected information about the connected cell's technology (e.g. LTE) and the geolocation of the measurements.

Ground truth	Total	FCC		Skyhook	
		NC	C	NC	C
NC	266	19%	81%	32%	68%
C	1,440	0%	100%	5%	95%

(a) Verizon

Ground truth	Total	FCC		Skyhook	
		NC	C	NC	C
NC	324	6%	94%	21%	79%
C	1,361	0%	100%	5%	95%

(b) T-Mobile

Ground truth	Total	FCC		Skyhook	
		NC	C	NC	C
NC	568	25%	75%	53%	48%
C	1,095	2%	98%	7%	93%

(c) AT&T

Ground truth	Total	FCC		Skyhook	
		NC	C	NC	C
NC	231	96%	4%	99%	2%
C	1,122	21%	79%	20%	80%

(d) Sprint

Table 5: Confusion matrices comparing ground truth coverage with FCC and Skyhook. NC denotes no LTE coverage and C denotes LTE coverage. Total denotes the number of ground measurements in each category.

This information is used to infer whether LTE coverage exists at a location. We consider LTE to be available if the *Service State* shows IN_SERVICE to indicate an active connection, and if the associated cell is an LTE cell. We term this the *ground truth* LTE coverage. We then compare the FCC and Skyhook coverage with the ground truth LTE coverage to see whether the two datasets agree. Note that we use the coverage shapefiles for both Skyhook and the FCC in this comparison instead of the census block centroid approach in Section 3.1.1. This allows us to compare coverage more precisely, especially if a census block is only partially covered. **Results:** Table 5 shows the confusion matrices that compare ground truth LTE coverage with reported coverage from the FCC and Skyhook maps. Both maps show coverage at locations where ground truth did not. In the case of Verizon, 81% of the measurements with no coverage are from locations reported as covered by the FCC. This over-reporting is lowest for Sprint and highest for T-Mobile.

We also observe significant disagreement (up to 79%) between Skyhook coverage and the ground truth. Two possibilities may cause this: i) paucity in Skyhook UE signal strength readings available for cell location and coverage radius estimation, or ii) error in the cell propagation model itself possibly due to variations in the environment conditions such as the terrain. In either case, Skyhook agrees better with the ground truth than the FCC in reporting areas with

no LTE coverage. In the case of AT&T, 75% of ground measurements with no LTE coverage belong to areas reported as covered by the FCC as compared to 48% by Skyhook.

4 MAPPING & MEASURING COVERAGE

Our analysis thus far finds that existing, widely-used datasets for LTE coverage in the United States contain regions of disagreement when compared to one another and to ground truth measurements. For example, in Section 3.1, we observe that coverage reports by both the FCC and Skyhook are prone to overestimation errors, likely a result of optimistic propagation models used to construct coverage estimates. End-user measurements remain the most accurate way to assess coverage. However, end-user measurements, especially via controlled active experiments, are cost and labor intensive, and hence are practical only when used sparingly.

Rather than dismissing the use of active end-user measurements out of hand, we propose to use (imperfect) existing datasets to guide the selection of areas in which to conduct targeted measurements. We envision that existing datasets can be combined to reveal which areas offer the least evidence about either coverage or lack of coverage. Based on this intuition, we present a Targeted Active Measurement Framework (TAMF) that assumes a limited budget for active measurements in a region and provides a sequence of sub-regions where active measurements should be performed with the goal of maximizing the value of a measurement campaign.

TAMF is driven by the observation that the utility of performing active measurements in different locations is often highly variant. This difference largely stems from two factors. First, information about coverage already exists in datasets with a varying degree of reliability depending on factors such as assessment methodology (e.g., end-user measurements vs. propagation modeling), data collection accuracy (e.g., measurement or positioning errors), and spatial context (e.g., urban vs. rural, open spaces vs. dense cover). Second, the value of knowing coverage in an area is inherently variable. Knowledge about human-inhabited or frequently accessed areas (i.e., along popular hiking or driving paths) is likely more broadly useful than knowledge about less accessible areas such as forests or water bodies.

TAMF utilizes this spatial variance in the utility of coverage data to target high-value knowledge areas to make good use of limited resources for measurements. In the rest of the section, we present the algorithmic components of TAMF integrated with a practical demonstration of building a measurement route through an area of varied coverage knowledge.

4.1 TAMF Model Overview

TAMF uses a grid-based model and divides a geographic region G into blocks of size $L \times L$. Each block i has an associated

“evidence of coverage” value (EoC_i) based on information from current datasets, and a value of knowing whether it is covered (VoC_i) defined as follows:

- Evidence of Coverage (EoC): This is a value ranging from -1 to 1. The sign represents whether the evidence indicates the area is covered (+) or is not covered (-). The magnitude is a measure of certainty in the evidence. For example, an EoC value approaching 1 indicates *very high* evidence that a grid block is covered; approaching -1 indicates *very high* evidence the block is *not* covered; and 0 indicates that existing evidence is not sufficient to make any claims whether the block is or is not covered. As we will discuss, the algorithm to construct EoC values from existing datasets is an interesting problem in its own right.
- Value of Coverage (VoC): This is a non-negative measure indicating the importance of knowing coverage for a grid block. VoC is determined by policy to reflect additional priorities of the measurement campaign. For instance, it may be more valuable to know about the coverage status in higher-population census blocks, or in low-income areas to assess the efficacy of disbursing funds to subsidize end-user connections.

This formulation assumes that all parts of a grid block are uniformly covered, and that making a measurement in the grid block suffices to reveal the ground truth in the block. This approximation becomes more accurate as block size is reduced, though finer grained block size results in longer running times to construct quality measurement campaigns.

We define the *utility* of measuring in a block i as follows:

$$u_i = VoC_i \times (1 - |EoC_i|)$$

If all grid blocks are equally valued, then the utility is highest where the absolute value of evidence of coverage is lowest, i.e., the evidence is least definitive.

A measurement campaign consists of a sequence of grid blocks where active measurements will be taken. We assume a single campaign that makes a measurement in a block then travels to the next block in the sequence. We assume that the *cost* of the campaign is the sum of the time required to visit each grid block in the sequence. Other costs associated with a campaign may include the time to perform the measurements and the cost of equipment including SIM cards and access plans. The human costs scale roughly with the distance traveled while the equipment costs are reasonably assumed constant for the length of campaigns we consider (hours rather than weeks).

We consider the case where the total budget of the measurement campaign is limited by some resource budget, B . Our goal is to find a sequence of grid blocks at which to perform measurements such that the *utility* of gathering coverage evidence is maximized while the *cost* of measurement is within budget.

Algorithm 1: CCTSP heuristic from [54]

Result: Subtour of blocks within budget B .
Initialize: manually set desired starting block(s);
for each block not yet in subtour **do**
 Prioritize remaining blocks by selection criteria;
 Randomly select a block from top T ;
 Insert into subtour at point of least cost;
 if budget is exceeded **then**
 Delete block with lowest utility/cost ratio;
 Reorder subtour into 2-opt arrangement;
for each block not yet in subtour **do**
 Prioritize remaining blocks by utility/cost ratio;
 if block can be inserted within budget **then**
 Insert into subtour at point of least cost;
 Reorder subtour into 2-opt arrangement;
for each block not yet in subtour **do**
 Prioritize remaining blocks by utility only;
 Insert into subtour at point of least cost;
 if budget is exceeded **then**
 Delete lowest-utility block so subtour cost is under budget;
Return subtour;

This problem formulation maps to a variant of the traveling salesman problem referred to as the cost-constrained TSP (CCTSP) where the goal is to select a *subtour* of cities (nodes with assigned values) that achieves maximum overall subtour value without exceeding a cost constraint [54]. CCTSP may select only a *subset* of all possible nodes to visit, so many established heuristic solvers for TSP (which find a tour visiting all nodes) do not directly apply to this constrained NP-hard problem. We use a greedy heuristic proposed by Sokkappa et al. [54] that borrows ideas from two earlier heuristics and improves upon them³.

Algorithm 1 shows the heuristic logic where candidate nodes are *blocks* and node value is *utility*. The first block or blocks of a subtour are set manually, indicating a desired starting position or forcing a visit to a particular block. The subtour is then built up by successively adding high-priority blocks within budget until every element in the dataset is either part of the subtour or has been discarded. Between passes, a standard 2-optimal (2-opt) rearrangement technique interchanges the order of any two segments of the subtour until the overall cost cannot decrease any further.

In the first pass, blocks are prioritized by a *selection criteria* proportional to an aggregate value score which adjusts the value of the current block with a weighted sum of all neighboring blocks. A block is selected randomly from the T blocks with the highest selection criteria value, then added to

³In the remainder of this subsection, we briefly describe the intuition behind this heuristic and refer the reader to the Sokkappa technical report for an in-depth explanation. We describe our modifications to the heuristic to reduce runtime in Section 4.3.

Provider	# of scan logs	# of cells
Verizon	21,241	949
T-Mobile	272,710	668
AT&T	54,506	525
Sprint	6,349	615

Table 6: Number of scan logs and cells observed in the crowd-sourced dataset in the grid.

the subtour. If the cost of adding this block overruns the budget, the block with the lowest value-to-cost ratio is discarded from the subtour and from consideration for the remainder of this pass. The second pass through all blocks not yet added to the subtour prioritizes nodes by the utility-to-cost ratio before either adding to the subtour or discarding immediately. The third pass prioritizes blocks only by utility, adds the next highest to the subtour, and discards the lowest currently in the subtour when the budget is exceeded.

4.2 EoC Map Construction

To use the TAMF Model requires construction of an EoC map from grid blocks to evidence of coverage values, and a VoC map from grid blocks to value of coverage. VoC is a matter of policy. In this section, we will describe three possible ways to construct EoC maps by leveraging existing datasets. None of these maps are *prima facie* better than the others, thus we also develop a methodology to evaluate the quality of an EoC map using ground truth. Obviously ground truth data would not generally be available; the point of the methodology is to define what it means for an EoC map to be “good” and to examine how the mapping methods compare in a region where we have ground truth data to inform method choice in other regions. Finally, we will evaluate the quality of the constructed EoC maps using our active measurement dataset collected within a region of New Mexico.

4.2.1 EoC Map Creation. We present three methods of EoC map construction using existing coverage datasets. These methods differ in their sources of evidence and how they use that evidence. Our goal in this section is to highlight plausible methods for construction of an EoC map to demonstrate its utility. We believe there is opportunity for much additional work on EoC map construction.

- **Map 1:** We first consider both the FCC and Skyhook coverage datasets as primary and equal sources of evidence. In this method, the EoC value for a grid block is assigned as 1 (-1) if both datasets agree that it is (not) covered, and 0 if they disagree.
- **Map 2:** We now consider the Skyhook coverage dataset and computed cell locations as primary evidence for coverage and the FCC dataset as evidence for no coverage. We use an additional insight that areas closer to the cell location are more likely to be covered than areas that are farther away. We divide the grid blocks covered by a cell

with a coverage radius r into five different regions based on their relative distance from estimated cell location. A grid block covered by a cell station is assigned EoC of 1 if it contains the cell, 0.8 if it is within $0.25 \times r$ distance from the cell, 0.6 if within $0.5 \times r$, 0.4 if within $0.75 \times r$, and 0.2 otherwise. EoC is assigned to be -1 if the grid block is not covered by both Skyhook and FCC. The remaining grid blocks are assigned an EoC value of 0.

- **Map 3:** We augment *Map 2* with an additional source of evidence, i.e., the scan logs from crowdsourced measurements. We also use the signal strength value of the scan log as an evidence of coverage for neighboring grids. A high signal strength value likely indicates good coverage in the region. Thus, we update *Map 2* in two ways, i) assign an EoC value of 1 to all grid blocks where a scan log is observed, and ii) if a grid block has a scan log with *good* ($> -70\text{dBm}$) signal strength [1], increase the EoC value of each neighboring grid by 0.2, if it is non-negative. If the neighboring grid has an EoC value of -1, it is set to 0.

4.2.2 Quality of an EoC Map. We now turn to defining what it means for an EoC map to be “good.” We do so with a metric called the *accuracy score* that reflects the quality of an EoC map generation method by reference to underlying truth about coverage.

The *accuracy score* for a method is determined based on the following intuition: accuracy increases (decreases) when the evidence for a grid block turns out to be correct (wrong). The increase (decrease) depends on the magnitude of the EoC. The idea is that a method should be awarded (or penalized) in proportion to how strongly it claims coverage (or lack of coverage) at a particular block. The overall accuracy score is the sum taken over all blocks.

Formally, a grid block with ground truth coverage information and an evidence EoC_i has a score of $|EoC_i|$, if the estimation of coverage state is correct and $-n \times |EoC_i|$, if it is incorrect. The accuracy score of an EoC map is then defined as the sum of accuracy scores of all grid blocks. Here, n is a penalty factor for incorrect estimation and is ≥ 1 . It enables asymmetric scoring by penalizing a method more for being incorrect. This can be used to avoid methods that can otherwise gain a higher score due to biases in the underlying data. For instance, consider two EoC mapping methods evaluated using 10 grid blocks out of which 8 have coverage. The first method assigns an EoC value of 1 to all grid blocks while the second method assigns an EoC value of 1 to only 4 of the covered blocks and 0 to the remaining blocks. In absence of a penalty factor, the accuracy score for the first and the second method is 6 and 4, respectively. However, it makes more sense to use the second EoC map even though

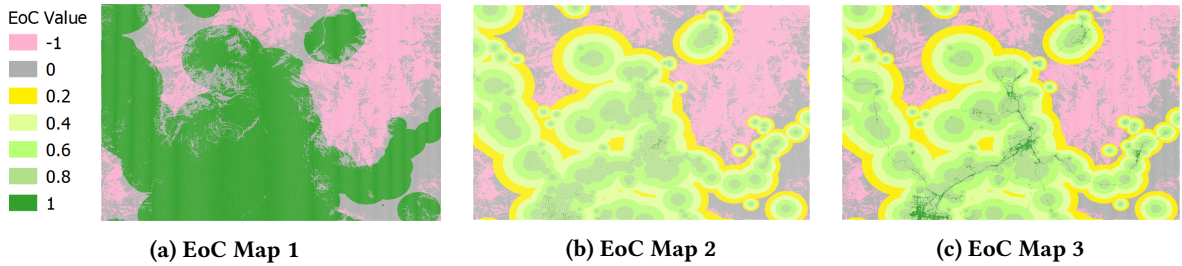


Figure 5: EoC Maps for Verizon created using different methodologies

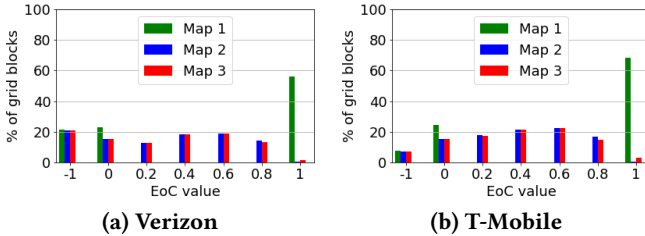


Figure 6: EoC value distribution for different EoC maps.

it has a lower accuracy score. Using a penalty factor (>1) for incorrect estimation can thus reduce the impact of this bias⁴.

4.2.3 Case Study. We now apply the EoC map creation methodologies described in Section 4.2.1 to a rectangular grid in northwestern New Mexico. The grid is centered around Santa Clara Pueblo with opposite corner points at $(36.52494, -107.19396)$ and $(35.15770, -104.94642)$ and an area of $30,798\text{km}^2$. We consider this region as we have ground truth logs from our active measurement campaign within a part of this region (see Section 2.3). We use it to evaluate the *accuracy score* of the *EoC* maps. Both FCC and the Skyhook coverage datasets as well as the Skyhook scan logs are used for generating the EoC maps. Table 6 shows the number of scan logs and cells per network provider as observed in the Skyhook dataset. The number of scan logs is highest for T-Mobile and lowest for Sprint. This could be either an artifact of the dataset collection or difference in popularity (or availability) of providers in the region. We consider grids of size $250m \times 250m$ for this analysis. This is similar to the block size proposed by the Rural Wireless Association in a recent measurement campaign in Oklahoma Panhandle [51]. **Results:** Figure 6 shows a distribution of the EoC values for Verizon and T-Mobile. Figure 5 shows a visualization of the EoC maps for Verizon. For both network providers, *Map 1* has the greatest number of blocks with EoC values of zero (see Figure 6). *Map 2* and *Map 3* have similar EoC value distributions. However, *Map 3* has a higher proportion of blocks with an EoC value of 1. These correspond to blocks for which a scan log was observed. We find that most of

⁴Sampling grid blocks within the ground truth data to balance *covered* and *not covered* blocks is another way to mitigate this bias. However, this may severely reduce the total number of grid blocks available for evaluating *accuracy score* in case of high imbalance

Provider	Num blocks	Accuracy Score					
		Map 1		Map 2		Map 3	
		n = 1	n = 2	n = 1	n = 2	n = 1	n = 2
Verizon	455	244	145	188.2	117.4	320	248
T-Mobile	449	355	310	276.6	248	346.8	314.6
AT&T	447	161	54	128.4	62.4	177	96.4
Sprint	533	504	502	433.2	430.4	458.2	446.4

Table 7: Accuracy score for different EoC maps.

these grid blocks are concentrated around urban areas and along major highways.

We evaluate the accuracy score of the three EoC maps using the ground truth data from our active measurement campaign. Table 7 shows the accuracy score for different providers. The *Num blocks* column indicates the number of grid blocks for which we have the ground truth. It is also the maximum possible score for any EoC map. We show the accuracy score for each map type under two cases, i.e., when the penalty factor, n , is 1 and 2. We observe that *Map 1* shows the highest accuracy score in two out of four providers when the penalty factor is 1. However, with the penalty factor increased to 2, it has the highest accuracy score in only one out of four providers. In this case, *Map 3* has the highest score in three out of four providers.

To understand the cause, we consider the percentage of errors for these maps for different EoC values for Verizon and T-Mobile (results from the other providers are similar). As shown in Figure 7, all three EoC maps have *zero* error in identifying grid blocks that are *not covered* but have different overestimation errors. *Map 1* has the highest error rate (up to 23%) for EoC values of 1 which can be attributed to the binary mapping of EoC values in this map. Therefore, its accuracy score is impacted the most when the penalty factor is increased. Thus, with a higher penalty factor, the gains that *Map 1* had resulting from the bias in the underlying active measurement dataset (higher proportion of *covered* blocks) and the binary mapping diminish significantly.

We also observe an interesting trend for both *Map 2* and *Map 3*, i.e., the error rate decreases as the EoC value increases for both the maps. This suggests that blocks that are further away from the cell have a higher chance of being misclassified as *covered*. This decreasing trend in error rate as the

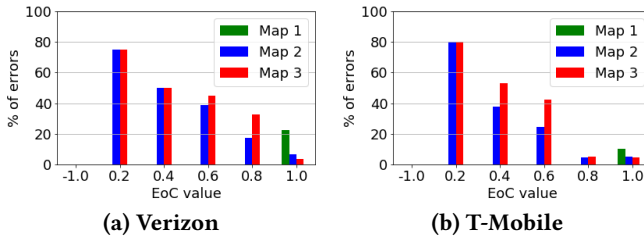


Figure 7: Percentage error for different EoC values.

EoC value increases is a desirable property in an EoC mapping method as higher EoC value blocks are less likely to be considered for active measurements. We also note some differences between *Map 2* and *Map 3*, as the former shows lower error rates for EoC values of 0.6 and 0.8, but a higher error rate for a value of 1. This is because of a combination of using scan logs to update the EoC value in a block and using signal strength to update the EoC value of neighboring blocks. We plan to understand the impact of both these factors in detail in our future work.

4.3 Maximizing Campaign Utility

In this section we demonstrate using the CCTSP heuristic to plan a measurement campaign using EoC *Map 3* to improve our knowledge of Verizon coverage. The campaign aims to maximize the utility (i.e., prioritize high-population areas where little coverage information is currently available) of new ground truth measurements while keeping within a limited resource budget.

Cost, budget, and utility: In this demonstration the *cost* of traveling between any two grid blocks is the travel duration in minutes between the centroid coordinates of each grid block. This duration is estimated by finding the Euclidian distance between each pair and dividing by the average New Mexico speed limit⁵, approximately 68 km/h (42.5 mi/h).

The constraining resource that determines budget is then the desired total duration of campaign travel in hours. We associate the VoC for a block with its population, calculated from the FCC census block dataset, where all grid blocks whose centroids fall within a census block are assigned that census block's population value [7]. Populations are then binned into a small number of exponentially increasing categories. Blocks with population 0 have *VoC* = 1; population 1–9 have *VoC* = 2; population 10–99 have *VoC* = 3; and population 100–999 have *VoC* = 4, and so on.

Reducing runtime complexity: Although the CCTSP heuristic runs in polynomial time, our New Mexico dataset has more than 557,000 grid blocks. By comparison, the dataset used by Sokkappa had 20–100 nodes. Using the standard heuristic resulted in unacceptably long run times. Given that

our goal here is to qualitatively demonstrate the feasibility and usefulness of our framework as opposed to actually perform a targeted measurement campaign, we make a few modifications in our evaluation setting. We reduce the geographic scope of consideration by randomly sampling 1% of the blocks. This reduces the the dataset to about 5K blocks with a utility value varying between 0 and 4. We then discard the blocks with zero utility (i.e., where coverage is already evident from one or more sources) before running the subtour, which further reduces the input dataset to 4,414 blocks. Finally, we modify the heuristic, specifically the aggregate value scoring process used in the selection criteria, to limit the number of neighboring blocks considered when scoring a single block, as described below.

Each block i in the dataset of n blocks is assigned an aggregate value score which is a function of its own utility and the sum of the utilities of every neighboring block j weighted through a decaying exponential by a constant scale factor μ and the cost c_{ij} to travel from block i to j .

$$\text{score}_i = u_i + \sum_{j=0, j \neq i}^{n-1} u_j \times e^{(-\mu \times c_{ij})}$$

This allows the heuristic to prioritize blocks within high-utility clusters and produce a more valuable subtour. The constant μ scales the weighting to the scope of the problem, so we use the author's default of $10/c_{max}$, where c_{max} is the maximum travel time in our dataset, i.e., 230 minutes.

The original heuristic uses all $n - 1$ nodes that remain to be considered (i.e., have not been added to or removed from the subtour) for calculating score_i . Since the set of remaining nodes changes every time the subtour is updated, this leads to the selection criteria to be recalculated on every update, causing the first pass through all blocks to take $O(n^2)$ time. In our adaptation for larger datasets, we limit the number of blocks considered neighbors by a maximum traveling cost. Instead of summing j over all other $n - 1$ blocks in the dataset, we consider as neighbors only blocks that are within some cost z away from block i . With $z = 10$ minutes, we allow on average 70 neighbors for any given block's aggregate score calculation, reducing the run time to $O(n)$.

The above modifications reduce our subtour generation time significantly. For instance, it takes around 1 minute for generating a subtour for an 8-hour budget and 2.5 minutes for a 16-hour budget on a machine using an Intel i7-8550U / 16 GB RAM and running Python 3.7.3.

Results: To demonstrate the variation possible in subtours generated over a single map, we use Verizon *Map 3* and select 10 of the highest utility blocks as starting blocks for our tour. Following the method described by Sokkappa, we introduce five *focus points* (FP), blocks located at the centroid of the dataset and at the centroids of each quadrant in the dataset. Each FP is added as a second initial block to a different subtour to force exploration throughout the entire map. With

⁵<https://www.safemotorist.com/NewMexico/Roads/speed.aspx>

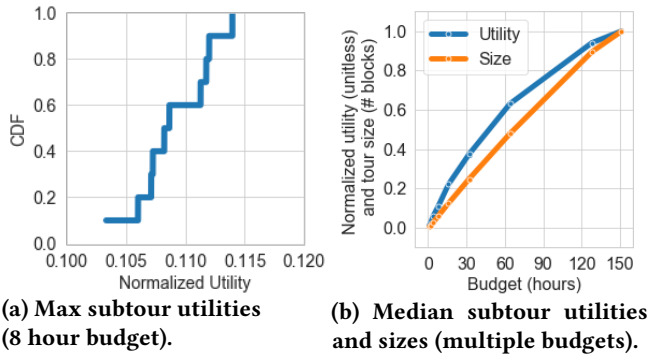


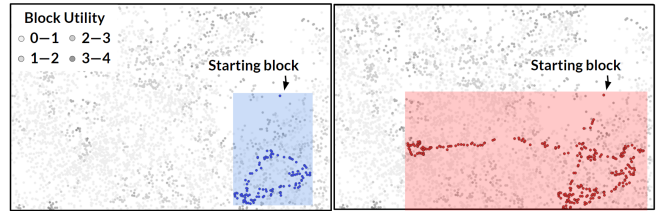
Figure 8: Subtour utilities for *Verizon Map 3*.

an 8-hour budget, we then generate five tours for each starting block and FP pairing, where the starting block may not be moved from the beginning of the tour, but the FP may be rearranged within the tour so long as it is not removed. Figure 8a shows the variation in the highest-utility subtours from each starting node, picked from 25 tours. The subtour utilities are normalized by dividing with the total sum of all block utilities, i.e., 4,180.

We then set the starting block to the highest-utility block on the map (located in the upper right quadrant) and run 100 subtours with budgets ranging from 1 hour to 151 hours, a manually determined budget which visits all 4,414 blocks in the dataset. To reduce the run-time complexity, especially for greater budgets, we consider subtours for only a single focus point, i.e., the lower-right quadrant.

Figure 9 shows two sample campaigns from these runs with budgets of 4 and 8 hours, respectively. The grey points represent the spatial location of the blocks and the intensity of the color represents the utility with darker grey corresponding to higher utility. A bounding box including all blocks in the sample 4-hour campaign covers an area of $4,096m^2$ (see Figure 9a). The bounding box of the 8-hour campaign covers an area of more than three times that size at $13,472m^2$ (see Figure 9b), and crosses into a high-utility cluster of blocks in the neighboring lower-left quadrant. These examples visually confirm that the heuristic prioritizes high-utility blocks. We also find that the blocks with higher utility (dark grey points in Figure 9) are unevenly distributed. These blocks correspond to high population areas where little coverage information is available. This suggests that measurement costs can also be reduced by considering multiple campaigns starting from different points as opposed to a single campaign. We plan to consider the implications of parallel campaigns on this tour-planning heuristic as a part of our future work.

We then examine the variation in utility from subtours generated from a range of budgets. Figure 8b shows the median normalized utility of 100 subtours for each budget up to 151 hours. The variation in subtour utility for the same



(a) 4-hour campaign with normalized utility of 0.06. (b) 8-hour campaign with normalized utility of 0.11. Figure 9: Sample tours on *Verizon Map 3* with single starting block and lower-right focus point.

budget is quite small, less than 0.0016, for all budgets. This is to be expected from setting the same starting and focus points for each subtour, as the heuristic tends to eventually settle on the same sets of high-utility nodes. More interestingly, the concave diminishing return between utility and budget is evident compared to the more linear increase in the size of the subtour, i.e., the incremental gain in subtour utility decreases as the budget is increased incrementally. This shows that TAMF is able to utilize the resource budget efficiently by prioritizing blocks with higher utility.

5 RELATED WORK

Measuring fixed broadband: Internet delivered to residence or business locations via technologies such as fiber and copper [11] and with a minimum speed of 25 Mbps (download) and 3 Mbps (upload) is classified as *fixed broadband* [17]. The FCC releases annual reports [10, 13–15, 17] based on network operator data [20] describing broadband availability across the United States, with the latest report (May 2019) claiming that over 25% of the Americans who lacked broadband access in 2016 had been reached by commercial operators in 2017 [10]. However, these reports have received numerous criticisms from independent organizations, questioning their accuracy especially in rural areas [23–25, 33, 38]. For instance, Meinrath et al. published a report showing that broadband access in Pennsylvania is actually much lower than claimed, drawing evidence from a public dataset of speed tests made available by M-Lab [38]. While an accurate characterization of fixed broadband access is also needed, the focus of this paper is on characterizing LTE access by combining multiple datasets.

Measuring mobile broadband: High-speed Internet access through cellular networks like LTE is classified as *mobile broadband* [17]. While the FCC has not defined a strict threshold for mobile broadband speeds, it currently uses a minimum speed of 5 Mbps/1 Mbps and a median speed of 10 Mbps/3 Mbps as a benchmark in its yearly reports of mobile LTE coverage [17]. As in the case of fixed broadband, various claims [3, 4, 23] have challenged the veracity of the FCC’s LTE coverage data [19]. However, most of these criticisms are either qualitative [23] or are limited in their

geographic scope as they involve obtaining ground measurements through wardriving [3, 4, 51]. Our goal in this paper is to evaluate the feasibility of using existing datasets, especially those obtained via crowdsourcing, to objectively assess LTE coverage at scale.

Crowdsourced datasets: Numerous datasets, both commercial [22, 53] and public [6, 39, 43, 44], provide information about cellular network infrastructure. Most of these datasets are constructed for device localization from cell tower measurements [59]. However, given that these datasets also contain information about LTE infrastructure, we believe they can be used to assess LTE coverage at scale and over time.

We use the Skyhook dataset [53] for our analysis. This dataset obtains network infrastructure information from crowdsourced end-user measurements. Various methods have been proposed to use these types of crowdsourced measurements to estimate the cell location [8, 35, 36, 42, 57, 60] and cell coverage [2, 52]. In this paper, we rely on the methodologies used by the respective datasets.

Ground truth measurements: Manual measurements have traditionally been a common approach to calculate cellular coverage [34]. This includes methods such as wardriving [27] and warwalking [56]. However, such methods require high operational expenditure, to such an extent that even network operators have considered use of crowdsourced user equipment measurements to assess coverage [26]. One of the goals of this paper is to understand whether and where crowdsourced datasets can be used for validating operator-provided coverage data, thus alleviating the need to perform expensive on-ground measurements.

Cost-constrained traveling salesman problem (CCTSP): Our approach to developing a measurement campaign schedule with constraints is related to the traveling salesman problem. Specifically, we must provide a solution to an NP-hard optimization problem given a resource budget and the ability to prioritize nodes and travel arcs based on the trade-off between the cost of inserting a new node into a tour and the overall value increase associated with visiting that node [5, 12, 32, 48, 54]. We approximate a solution to this variant by the heuristic proposed by [54], which prioritizes nodes for tour insertion with a neighborhood aggregate score that considers both node value and the values of nearby nodes.

6 DISCUSSION & FUTURE WORK

Limitations of sparse crowdsourced coverage data. While the fundamental goal of EoC mapping is to move beyond the limitations of sparse crowdsourced coverage data and models that overestimate LTE coverage, a key limitation for EoC mapping in rural areas is its reliance on sparse crowdsourced LTE coverage data. When very few devices are used to collect LTE coverage data, the accuracy of quality of service measurements such as signal strength is more likely to be skewed

by just a few uncalibrated UEs. This decreases the accuracy of tower locations and range estimations. While this sampling may impact EoC models that leverage coverage maps and tower locations generated from sparse crowdsourced data, we assume that a crowdsourced measurement of LTE coverage at a particular point in space sufficiently represents ground truth about coverage at that point (regardless of the specific QoS metrics). While these individual points may not be sufficient on their own to generate an accurate coverage map, we argue that they are good enough to confirm the accuracy of coverage maps in particular places (such as in *EoC Map 3*). While there is data about the true location of cell towers, it is a direction for future work to determine the density of crowdsourced LTE measurements required to accurately confirm a general coverage range for a particular tower located in a particular type of terrain.

Integrating additional data into EoC. The EoC mapping model was designed to accommodate the integration of additional data sources, including other crowdsourced LTE measurements and coverage maps [43, 44]. As communities collaborate to better characterize their cellular coverage, they may be able to contribute data with restricted access, such as specific cell tower locations, sector angles, and antenna positions. Moreover, the EoC model is not limited to mapping LTE, but can be a useful way to assess coverage offered by other wireless technologies such as 5G and LPWANs.

Variations in cost and utility. The TAMF presented in this paper uses a simple model for cost and utility, where cost approximates on-road driving time and utility is calculated proportional to the amount of new evidence that can be gained and the population associated with an area that should be measured. However, communities using EoC maps and the TAMF to design a measurement campaign can tailor cost and utility values to their own requirements. For instance, some communities may use fleets of aerial drones to collect LTE measurements over space [40], so they may decide to base cost on geodesic distances; other communities may decide they want to calculate utility based on the number of remote sensors that need to be placed in a particular area, and can update the calculation accordingly.

Tuning map accuracy. In Section 4.2, we presented three different EoC maps. Our future work will investigate alternative EoC map evaluation mechanisms. For example, an EoC map might be heavily penalized for overestimating evidence of coverage, but only minimally penalized for underestimating evidence of coverage; or only rewarded for correctly reporting evidence of coverage. By investigating new evaluative mechanisms for rewarding and penalizing EoC maps, we can develop EoC models that are more closely tuned to the budgets and purposes of the communities who would use them.

REFERENCES

- [1] Kareem Abdullah, Noha Korany, Ayman Khalafallah, Ahmed Saeed, and Ayman Gaber. 2019. Characterizing the Effects of Rapid LTE Deployment: A Data-Driven Analysis. In *Proc. of IEEE/IFIP TMA*.
- [2] Jørgen Bach Andersen, Theodore S Rappaport, and Susumu Yoshida. 1995. Propagation Measurements and Models. *IEEE Communications Magazine* (1995), 43.
- [3] Rural Wireless Association. 2018. RWA Calls for FCC Investigation of T-Mobile Coverage Data. (2018). <https://ruralwireless.org/rwa-calls-for-fcc-investigation-of-t-mobile-coverage-data/>
- [4] Rural Wireless Association. 2019. Mobile Wireless in Vermont. (January 2019). <https://publicservice.vermont.gov/sites/dps/files/documents/Connectivity/BroadbandReports/2019/MobileWirelessReport.pdf>
- [5] Benjamín Barán. 2001. Improved AntNet Routing. *SIGCOMM Computer Communications Review* 31, 2 (April 2001), 42–48.
- [6] CellMapper. 2019. CellMapper. (2019). <https://www.cellmapper.net/map>
- [7] Census Bureau. 2019. Urban-rural definition. (2019). <https://www.census.gov/programs-surveys/geography/guidance/geo-areas/urban-rural.html>
- [8] Yu-Chung Cheng, Yatin Chawathe, Anthony LaMarca, and John Krumm. 2005. Accuracy characterization for metropolitan-scale Wi-Fi localization. In *Proceedings of the 3rd international conference on Mobile systems, applications, and services*. ACM, 233–245.
- [9] Federal Communications Commission. 2017. Mobile Deployment Form 477 Data. (2017). <https://www.fcc.gov/mobile-deployment-form-477-data>
- [10] Federal Communications Commission. 2019. Broadband Deployment Report. <https://www.fcc.gov/reports-research/reports/broadband-progress-reports/2019-broadband-deployment-report>. (May 2019).
- [11] Federal Communications Commission. 2019. Fixed broadband technology codes. (2019). <https://www.fcc.gov/general/technology-codes-used-fixed-broadband-deployment-data>
- [12] Rundefinedzvan Cristescu and Martin Vetterli. 2003. Power Efficient Gathering of Correlated Data: Optimization, NP-Completeness and Heuristics. *SIGMOBILE Mobile Computing Communications Review* 7, 3 (July 2003), 2.
- [13] FCC. 2017. Mobile Broadband Deployment Data from Form 477. (2017). <https://www.fcc.gov/form-477-mobile-voice-and-broadband-coverage-areas>
- [14] Federal Communications Commission. 2015. Broadband Progress Report. <https://www.fcc.gov/reports-research/reports/broadband-progress-reports/2015-broadband-progress-report>. (February 2015).
- [15] Federal Communications Commission. 2016. Broadband Progress Report. <https://www.fcc.gov/reports-research/reports/broadband-progress-reports/2016-broadband-progress-report>. (January 2016).
- [16] Federal Communications Commission. 2017. Connect America Fund (CAF). <https://www.fcc.gov/general/connect-america-fund-caf>. (February 2017).
- [17] Federal Communications Commission. 2018. Broadband Deployment Report. <https://www.fcc.gov/reports-research/reports/broadband-progress-reports/2018-broadband-deployment-report>. (February 2018).
- [18] Federal Communications Commission. 2019. FCC centroid methodology. (2019). <https://docs.fcc.gov/public/attachments/DA-16-1107A1Rcd.pdf>
- [19] Federal Communications Commission. 2019. FCC Mobile Broadband Dataset. (2019). <https://www.fcc.gov/form-477-mobile-voice-and-broadband-coverage-areas>
- [20] Federal Communications Commission. 2019. Form 477 instructions document. (2019). <https://transition.fcc.gov/form477/477inst.pdf>
- [21] GeoPandas. 2019. Python library for geospatial operations. (2019). <http://geopandas.org/>
- [22] Google Geolocation API. 2019. Cell/WiFi-based localization. (2019). <https://developers.google.com/maps/documentation/geolocation/intro>
- [23] Government Accountability Office. 2018. BROADBAND INTERNET: FCC's Data Overstate Access on Tribal Lands. (September 2018).
- [24] Tony H Grubasic. 2012. The US national broadband map: Data limitations and implications. *Telecommunications Policy* 36, 2 (2012), 113–126.
- [25] Tony H Grubasic and Elizabeth A Mack. 2015. *Broadband telecommunications and regional development*. Routledge.
- [26] Wuri A Hapsari, Anil Umesh, Mikio Iwamura, Małgorzata Tomala, Bódog Gyula, and Benoist Sebire. 2012. Minimization of drive tests solution in 3GPP. *IEEE Communications Magazine* 50, 6 (2012), 28–36.
- [27] Chris Hurley, Russ Rogers, Frank Thornton, and Brian Baker. 2007. *Wardriving and Wireless Penetration Testing*. Syngress.
- [28] International Telecommunications Union. 2015. ICT Facts and Figures: The World in 2015. <https://www.itu.int/en/ITU-D/Statistics/Documents/facts/ICTFactsFigures2015.pdf>. (May 2015).
- [29] International Telecommunications Union. 2016. ICT Facts and Figures: The World in 2016. <https://www.itu.int/en/ITU-D/Statistics/Documents/facts/ICTFactsFigures2016.pdf>. (May 2016).
- [30] International Telecommunications Union. 2017. ICT Facts and Figures: The World in 2017. <https://www.itu.int/en/ITU-D/Statistics/Documents/facts/ICTFactsFigures2017.pdf>. (May 2017).
- [31] Internet Society. 2016. A Policy Framework for Enabling Internet Access. <https://www.internetsociety.org/resources/doc/2016/a-policy-framework-for-enabling-internet-access/>. (2016).
- [32] Matthias Joest and Wolfgang Stille. 2002. A User-Aware Tour Proposal Framework Using a Hybrid Optimization Approach. In *Proceedings of the 10th ACM International Symposium on Advances in Geographic Information Systems*. New York, NY, USA.
- [33] John Kahan. 2019. It's time for a new approach for mapping broadband data to better serve Americans. (2019). <https://blogs.microsoft.com/on-the-issues/2019/04/08/its-time-for-a-new-approach-for-mapping-broadband-data-to-better-serve-americans/>
- [34] Jaana Laiho, Achim Wacker, and Tomáš Novosad. 2002. *Radio network planning and optimisation for UMTS*. Vol. 2. Wiley Online Library.
- [35] Zhijing Li, Ana Nika, Xinyi Zhang, Yanzi Zhu, Yuanshun Yao, Ben Y Zhao, and Haitao Zheng. 2017. Identifying value in crowdsourced wireless signal measurements. In *Proceedings of the 26th International Conference on World Wide Web*. 607–616.
- [36] Hyuk Lim, Lu-Chuan Kung, Jennifer C Hou, and Haiyun Luo. 2005. *Zero-configuration, robust indoor localization: Theory and experimentation*. Technical Report.
- [37] Benoit Lubek. [n. d.]. ([n. d.]). <https://github.com/caarmen/network-monitor>
- [38] Sascha Meinrath, Hannah Bonestroo, Georgia Bullen, Abigail Jansen, Steven Mansour, Christopher Mitchell, Chris Ritzo, and Nick Thieme. 2019. *Broadband Availability and Access in Rural Pennsylvania*. Technical Report. Pennsylvania State University.
- [39] Mozilla Location Service. 2019. Cell/WiFi-based localization. (2019). <https://location.services.mozilla.com/>
- [40] Michael Nekrasov, Vivek Ardash, Udit Paul, Esther Showalter, Morgan Vigil-Hayes, Ellen Zegura, and Elizabeth Belding. 2019. Evaluating LTE Coverage and Quality from an Unmanned Aircraft System. In *Proceedings of the 16th IEEE Conference on Mobile and Ad-hoc and Smart Systems*. Monterrey, CA, USA.
- [41] New Mexico Economic Development Department. 2019. New Mexico Climate & Geography. <https://gonm.biz/why-new-mexico/climate-geography>. (January 2019).

- [42] Petteri Nurmi, Sourav Bhattacharya, and Joonas Kukkonen. 2010. A grid-based algorithm for on-device GSM positioning. In *Proceedings of the 12th ACM international conference on Ubiquitous computing*. ACM, 227–236.
- [43] OpenCellID. 2019. OpenCellID Open Data. (2019). <https://opencellid.org/downloads.php>
- [44] Opensignal. 2019. About Us. <https://www.opensignal.com/about-us>. (January 2019).
- [45] Pew Research Center. 2019. Internet/Broadband Fact Sheet. <https://www.pewinternet.org/fact-sheet/internet-broadband/>. (June 2019).
- [46] Pew Research Center. 2019. Mobile Fact Sheet. <https://pewresearch.org-preprod.go-vip.co/pewinternet/fact-sheet/mobile/>. (June 2019).
- [47] James E Priefer. 2017. Mobile data roaming and incentives for investment in rural broadband infrastructure. Available at SSRN 3391478 (2017).
- [48] Robert Ricci, Chris Alfeld, and Jay Lepreau. 2003. A Solver for the Network Testbed Mapping Problem. *SIGCOMM Computer Communications Review* 33, 2 (April 2003), 65.
- [49] Elisabeth Roberts, David Beel, Lorna Philip, and Leanne Townsend. 2017. Rural Resilience in a Digital Society. *Journal of Rural Studies* 54 (2017), 355–359.
- [50] Laura Robinson, Shelia R Cotten, Hiroshi Ono, Anabel Quan-Haase, Gustavo Mesch, Wenhong Chen, Jeremy Schulz, Timothy M Hale, and Michael J Stern. 2015. Digital Inequalities and Why They Matter. *Information, Communication & Society* 18, 5 (2015), 569–582.
- [51] Rural Wireless Association. 2019. Challenges faced by small wireless providers in measuring LTE coverage. (2019). <https://ruralwireless.org/rwa-welcomes-fcc-investigation-into-violation-of-mobility-fund-phase-ii-mapping-rules/>
- [52] Noman Shabbir, Muhammad T Sadiq, Hasnain Kashif, and Rizwan Ullah. 2011. Comparison of radio propagation models for long term evolution (LTE) network. *arXiv preprint arXiv:1110.1519* (2011).
- [53] Skyhook. 2019. Coverage Area. (2019). <https://www.skyhook.com/coverage-map>
- [54] Padmini R Sokkappa. 1990. *The cost-constrained traveling salesman problem*. Technical Report. Lawrence Livermore National Lab., CA (USA).
- [55] David Tse and Pramod Viswanath. 2005. *Fundamentals of wireless communication*. Cambridge university press.
- [56] Arvin Wen Tsui Tsui, Wei-Cheng Lin, Wei-Ju Chen, Polly Huang, and Hao-Hua Chu. 2010. Accuracy performance analysis between war driving and war walking in metropolitan Wi-Fi localization. *IEEE Transactions on Mobile Computing* 9, 11 (2010), 1551–1562.
- [57] Alex Varshavsky, Denis Pankratov, John Krumm, and Eyal De Lara. 2008. Calibree: Calibration-free localization using relative distance estimations. In *International Conference on Pervasive Computing*. Springer, 146–161.
- [58] World Population Review. 2019. New Mexico Population 2019. <http://worldpopulationreview.com/states/new-mexico-population/>. (January 2019).
- [59] Jie Yang, Alexander Varshavsky, Hongbo Liu, Yingying Chen, and Marco Gruteser. 2010. Accuracy characterization of cell tower localization. In *Proceedings of the 12th ACM international conference on Ubiquitous computing*. ACM, 223–226.
- [60] Kiran Yedavalli, Bhaskar Krishnamachari, Sharmila Ravula, and Bhaskar Srinivasan. 2005. Ecolocation: a sequence based technique for RF localization in wireless sensor networks. In *Proceedings of the 4th international symposium on Information processing in sensor networks*.